Open Access Full Text Article

ORIGINAL RESEARCH

Size and PEG Length-Controlled PEGylated Monocrystalline Superparamagnetic Iron Oxide Nanocomposite for MRI Contrast Agent

Li-Hua Deng [ID][1,2]
Hai Jiang[1]
Fu-Lin Lu[1]
Han-Wei Wang[1]
Yu Pu[1]
Chang-Qiang Wu [ID][1]
Hong-Jie Tang[3]
Ye Xu[4]
Tian-Wu Chen[1]
Jiang Zhu[1]
Cheng-Yi Shen[1]
Xiao-Ming Zhang[1]

[1]Medical Imaging Key Laboratory of Sichuan Province and School of Medical Imaging, Affiliated Hospital of North Sichuan Medical College, Nanchong, 637000, People's Republic of China; [2]Department of Radiology, First People's Hospital of Neijiang, Neijiang 641000, People's Republic of China; [3]Department of Radiology, Nanchong Hospital of Traditional Chinese Medicine, Nanchong 637000, People's Republic of China; [4]Department of Radiology, Children's Hospital of Chongqing Medical University, Chongqing 401122, People's Republic of China

Correspondence: Chang-Qiang Wu;
Xiaoming Zhang
Sichuan Key Laboratory of Medical Imaging and School of Medical Imaging, Affiliated Hospital of North Sichuan Medical College, 234th Fujiang Road, Nanchong 637000, People's Republic of China
Tel +86-13990723836
Email wucq1984@163.com;
zhangxm@nsmc.edu.cn

Objective: PEGylated superparamagnetic iron oxide (SPIO) is the most promising alternatives to gadolinium-based contrast agents (GBCAs) in MRI. This paper is to explore the imaging effects of PEGylated SPIO, which is influenced by particle sizes and surface polyethylene glycol (PEG) coating, using as MRI contrast agents at different magnetic field intensities.

Methods: Firstly, nine PEGylated monocrystalline SPIO nanoparticles with different nanocrystal sizes and different molecular weights PEG coating were prepared, and then physical and biological properties were analyzed. Finally, MRI imaging in vivo was performed to observe the imaging performance.

Results: Nine PEGylated monocrystalline SPIO nanoparticles have good relaxivities, serum stability, and biosecurity. At the same time, they show different imaging characteristics at different magnetic field intensities. Eight-nanometer SPIO@PEG5k is an effective T_2 contrast agent at 3.0 T ($r_2/r_1 = 14.0$), is an ideal T_1-T_2 dual-mode contrast agent at 1.5 T ($r_2/r_1 = 6.52$), and is also an effective T_1 contrast agent at 0.5 T ($r_2/r_1 = 2.49$), while 4-nm SPIO@PEG5k is a T_1-T_2 dual-mode contrast agent at 3.0 T ($r_2/r_1 = 5.24$), and is a useful T_1 contrast agent at 0.5 T ($r_2/r_1 = 1.74$) and 1.5 T ($r_2/r_1 = 2.85$). MRI studies in vivo at 3.0 T further confirm that 4-nm SPIO@PEG5k displays excellent T_1-T_2 dual-mode contrast enhancement, whereas 8-nm SPIO@PEG5k only displays T_2 contrast enhancement.

Conclusion: PEGylated SPIOs with different nanocrystal sizes and PEG coating can be used as T_1, T_2, or T_1-T_2 dual-mode contrast agents to meet the clinical demands of MRI at specific magnetic fields.

Keywords: magnetic resonance imaging, contrast agents, superparamagnetic iron oxide, polyethylene glycol

Introduction

Gadolinium-based contrast agents (GBCAs) are widely used in clinical magnetic resonance imaging (MRI). In recent years, however, their safety has been under great concern, due to the associated nephrogenic system fibrosis (NSF) and gadolinium retention.[1–3] Superparamagnetic iron oxides (SPIO) have been widely studied as MRI contrast agents for many years, because of their excellent magnetic properties and biocompatibility.[4–7] SPIO-based nanoparticles demonstrate high proton relaxation efficiency and slower kidney clearance, which can be used at low concentrations compared with GBCAs.[8] Meanwhile, iron, as the main component, is also one of the essential elements within the human body, and hence has

inherent metabolic pathways in vivo. Therefore, SPIO may be considered as the most promising alternative to GBCAs in MRI.

SPIOs are small-sized iron oxide nanocrystals (Fe_3O_4 or γ-Fe_2O_3). To obtain the colloidal stability of these inorganic nanocrystals in biological applications, surface coating with water-soluble materials is essential.[4–7] Polyethylene glycol (PEG) is the most commonly used non-ionic hydrophilic polymer with good biocompatibility and has been widely applied in biopharmaceuticals as a solvent or excipient.[9] PEGylation of biomolecules or drug delivery nanocarriers can increase the circulatory half-life, and reduce antigenicity as well as immunogenicity in vivo, hence improving its pharmaceutical and pharmacological properties.[10–12] Over the past decade, PEGylated SPIOs have been developed by various methods, and they exhibited favorable stability in aqueous phase and biocompatibility. For example, the amphiphilic polymer based on PEG (PCL-PEG or DSPE-PEG) can form micelles when in an aqueous phase and were used to encapsulate hydrophobic SPIO to form PEGylated SPIO nanoclusters.[13–15] The size of these PEGylated SPIO nanoclusters ranges from tens to hundreds of nanometers and can be tuned by adjusting the ratio between the polymer and SPIO. Another method to obtain PEGylated SPIO is to modify specific ligands at the end of PEG, which chelates iron (III) onto the surface of SPIO nanocrystals.[16–19]

Previous research has shown that SPIO nanoclusters usually have high T_2 relaxivity (r_2), and can only be used as T_2 contrast agents.[8] However, clinical applications of T_2 contrast agents were limited due to the 'black holes' effect, which makes it difficult to distinguish between contrast enhancement lesions and low signal-to-noise ratio (SNR) areas such as calcification, air, hemorrhage, and blood clots.[20,21] Monodisperse small-sized SPIO nanocrystals suppress the T_2 effect as a result of their small magnetic moment and maintain a high T_1 relaxivity (r_1). This kind of SPIO nanoparticles has been studied as T_1 or T_1-T_2 dual-mode contrast agents according to their r_2/r_1 ratio.[22,23] Therefore, PEGylated small-sized SPIO nanocomposites have important clinical application and research value.

The relaxivities (r_2 and r_1) and dynamic distributions of the SPIO nanoparticles in the body are of vital importance to its imaging effect in contrast-enhanced MRI (CEMRI) and are mainly related to the crystal size, crystal shape, surface coating, and aggregation state.[24–26] It is hence of great significance to systematically study the interactive relationship between the properties and parameters of PEGylated SPIO, to facilitate advances in its development

and potential applications. In this paper, we designed and prepared nine PEGylated monocrystalline SPIO nanoparticles with various nanocrystal sizes and surface PEG lengths (Figure 1A), and performed detailed studies of their relaxation properties in vitro and imaging features in vivo.

Materials and Methods
Synthesis of Dopamine-Modified Polyethylene Glycol (PEG-DA)

Polyethylene glycol methyl ether (mPEG-OH) with different molecular weights (Mn = 550, 2k, or 5k Da) were purchased from Sigma-Aldrich (St Louis, MO, USA). 1-mmol mPEG-OH was placed in a 100 mL round bottom flask, and vacuum dried for 2 h. 20 mL of dried tetrahydrofuran was added and stirred magnetically. Carbonyldiiazole (810 mg, 5 mmol) was added in an inert gas atmosphere, and the mixture was refluxed overnight. The resulting solution was cooled to room temperature by removing the heat source, and 100 μL of water was added and stirred for 5 min. Vacuum distillation was performed and the product obtained was dissolved in 20-mL dichloromethane, and dropped into cold diethyl ether to obtain the precipitate (mPEG-CI).

1-mmol mPEG-CI was dissolved in 40 mL of tetrahydrofuran. Dopamine hydrochloride (560 mg, 3 mmol) and triethylamine (1 mL) were added under an inert gas atmosphere and reacted at room temperature for 24 h. The solvent was evaporated using vacuum distillation. The product was dissolved in 20-mL dichloromethane, and dropped into cold diethyl ether to obtain the precipitate which was dried under vacuum conditions to give the white powdered product (mPEG-DA).

The Preparation of PEGylated SPIO Nanoparticles (SPIO@PEG)

SPIO nanocrystals were synthesized by thermal decomposition of iron acetylacetonate (Sigma Aldrich, St Louis, MO, USA), and the crystal size was tuned by modifying the reaction conditions (namely the reaction temperature and solvent) as previously reported.[27] The detailed procedures were described in Supporting Information. The citric acid (1 g) was dissolved in 70 mL of ultrapure water, and NaOH was added to adjust the pH as 7.2. One hundred and ten milliliter acetone and 70-mL SPIO hexane solution (containing 50-mg nanoparticles) were added. The mixture was stirred and refluxed for 48 h. The sodium citrate coated SPIO (SPIO@CA) was obtained by centrifugation after ligand exchange, and subsequently dispersed in ultrapure water.
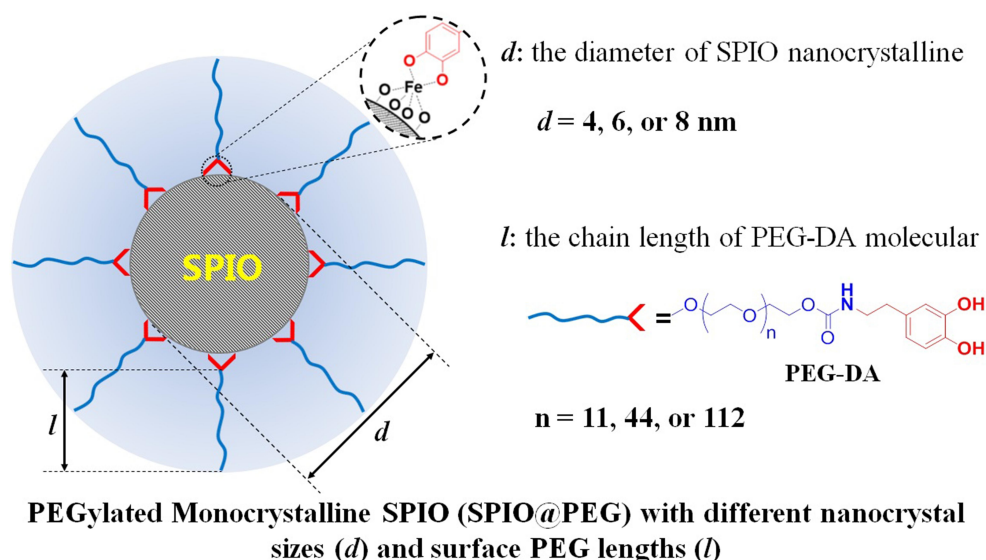
d: the diameter of SPIO nanocrystalline

$d = 4, 6,$ or 8 nm

l: the chain length of PEG-DA molecular

PEG-DA

$n = 11, 44,$ or 112

PEGylated Monocrystalline SPIO (SPIO@PEG) with different nanocrystal sizes (*d*) and surface PEG lengths (*l*)

Figure 1 Conceptual graph of PEGylated monocrystalline SPIO nanoparticles (SPIO@PEG) with various nanocrystal sizes (*d*) and surface PEG lengths (*l*). In our research, three SPIO crystal particles (4, 6, and 8 nm) and three PEG (Mn = 550, 2k, or 5k Da) were used to prepare nine SPIO@PEG nanoparticles.

Then, 150 mg of mPEG-DA (Mn = 550, 2k or 5k Da) and 5 mL of SPIO@CA solution (containing 10-mg nanoparticles) were mixed and magnetically stirred under a flow of nitrogen for 72 h at 40°C after being deoxidized. The solution was dialyzed against water for 2 days to obtain PEGylated SPIO (SPIO@PEG). The concentration of iron was determined using an atomic absorption spectrometer (AAS).

Relaxivity of SPIO@PEG Nanoparticles in vitro

The samples were diluted to different iron concentrations (0.05, 0.1, 0.2, 0.3, 0.4, and 0.5 mmol/L) and placed in test bottles. Longitudinal and transverse relaxation times (T_1 and T_2) were measured at room temperature at 0.5 T (by a 0.5 T magnetic resonance developer relaxation rate analyzer, Niumag, Shanghai, China), 1.5 T and 3.0 T (by clinical GE MRI systems, General Electric Company, Boston, Massachusetts, USA), respectively. Then, T_1 or T_2 relaxivity (r_1 or r_2) was calculated through the curve fitting of the relaxation rate ($1/T_1$ or $1/T_2$, s^{-1}) versus the iron concentration (mM).

Cytotoxicity of SPIO@PEG Nanoparticles

The mouse macrophage cell line RAW264.7 cells purchased from Procell (Wuhan, Hubei, China), were placed in 96 well plates at a concentration of 10×10^3 per well (100 μL), and cultured for 24 h in a humidified atmosphere containing 5%

of CO_2. Then, the cells were incubated for 24 h in a culture medium that included SPIO@PEG nanoparticles with different Fe concentrations (20, 15, 10, and 5 μg/mL). CCK-8 (10 μL/well) reagent (Bio Basic Inc, Konrad Cres, MO, Canada) was added under dark conditions. Absorbance was measured after 1 ~ 2 h, and the absorbance was determined using the microplate photometer. Cell viability was calculated using the following equation: Cell viability (%) = (N_s/N_c) × 100, where N_s and N_c are the absorbance of surviving cells treated with or without SPIO@PEG nanoparticles. The absorbance of media with or without SPIO@PEG nanoparticles was corrected and used as blank control for deduction.

Statistical Analysis

Data were presented as mean ± SD (Gaussian distribution) or median and IQR (Skewed distribution). Statistical analysis was performed with SAS 9.4 (Raleigh, North Carolina, USA). Weighted ANOVA was used for comparison between groups, and the SNK-q method was used for pair-wise comparison. Two-factor ANOVA was used for factorial design. When the interaction effects were statistically significant, intra-group and inter-group pair comparisons were further conducted, and the Bonferroni method was used to adjust P values. The results were considered statistically significant when p < 0.05.

Serum Stability Test

SPIO@PEG (8 mmol/L Fe concentration), volumetric fraction of 20% fetal bovine serum and PBS were placed

in 37°C water bath for 5 min, 1 h, 3 h, 5 h, and 24 h. 200-μL samples were added to 1-mL phosphate-buffered saline (PBS) in the colorimetric dishes, and finally the particle size distribution was detected by Malvern nanoparticle size and zeta potential analyzer (Malvern, England), respectively.

In vivo Imaging of Rats

All animal procedures were performed in accordance with the Guidelines for Care and Use of Laboratory Animals of North Sichuan Medical College and experiments were approved by the Animal Ethics Committee of North Sichuan Medical College (P20191226). MRI studies were performed with a GE 3.0T MRI scanner by using a rat coil for transmission and reception of the signal. Sprague Dawley (SD) rats (age: 6–8 weeks, weight: 200 g) were anesthetized by inhalational anesthesia systems, and an MRI scan performed before and immediately after injection, 1, 30, 60, 120 min and 24 h with the contrast agent administered at a dose of 5 mg (Fe)/kg body weight. Signal intensity (SI) was measured at each time point, and the change in the relative normalized signal intensities (NSI) was plotted against time. The MRI sequence and parameters were as follows.

Contrast-enhanced magnetic resonance angiography (CEMRA) imaging: TE = minimum, TR = 6.2 ms, FOV = 140 mm × 140 mm, slice thickness = 2.0 mm, and slice spacing = 0.6 mm, and flip angle 30°;

T_1-T_2 dual-mode imaging: T_1-mode (GRE sequence, TE = 3 ms, TR = 9 ms, flip angle 30°), T_2-mode (FSE sequence, TE = 76 ms, TR = 4.0 s, flip angle 142°), FOV = 80 mm × 80 mm, and slice thickness = 3.0 mm;

T_2 mapping: FSE sequence, TE = 8, 16, 24, 31, 39, 47, 55, 63 ms, TR = 1.2 s, FOV = 80 mm × 80 mm, slice thickness = 2.0 mm, slice spacing = 0.6 mm, and flip angle 90°.

After MRI scan, the rats were kept for another 4 weeks and their mental states, activities and feeds were observed. No abnormalities were found and none of them died in the end, which suggested that SPIOs have no toxicity to rats indirectly.

Results
Synthesis of PEG-DA

Catechol-group modified PEG (PEG-DA) was synthesized by a two-step chemical modification of mPEG-OH. The terminal hydroxyl group of mPEG-OH was activated by

reaction with 1,1′-carbonyldiimidazole, and then the activated intermediate reacted with the amino group of dopamine to obtain PEG-DA (Figure S1). Three molecular weights mPEG-DA (550 Da, 2k Da and 5k Da) were prepared in this work, and the corresponding ^{1}H NMR spectra can be found in the supporting information (Figures S2–S7).

Synthesis of SPIO Nanocrystals with Various Crystal Sizes

SPIO nanocrystals with high-quality were synthesized by high-temperature thermal decomposition, and the crystal size was tuned by changing the reaction solvent and heating conditions. The crystal size and dispersity were examined using transmission electron microscopy (TEM) and dynamic light scattering (DLS). As shown in Figure 2A, three SPIO nanoparticles displayed favorable monodispersity in TEM, and the lattice fringes were clearly visible in the high-resolution TEM (HRTEM) images. The crystal sizes were measured by selecting different representative areas under the TEM and were 3.7 ± 0.7 nm (4-nm SPIO), 5.2 ± 1.2 nm (6-nm SPIO), and 6.7 ± 0.9 nm (8-nm SPIO), respectively. In the DLS analysis, the SPIO nanoparticles show narrow particle size distribution in hexane (PDI: 0.421, 0.356 and 0.283 for 4 nm, 6 nm and 8 nm SPIO nanoparticles, respectively), and there is a slight increase in the average size (4.4 ± 3.0 nm, 11.2 ± 6.0 nm and 16.0 ± 10.0 nm, respectively) due to the surface organic molecular layer. Selected area electron diffraction (SAED) patterns of this SPIO nanocrystals are shown in Figure S8a–S8c. The measured lattice spacing based on the rings in the diffraction pattern conformed to the known lattice spacing for Fe_3O_4 crystal (Figure S8d).

Synthesis of PEGylated SPIO with Different Crystal Sizes and PEG Lengths

SPIO nanoparticles were transferred to the aqueous phase by ligand exchange with sodium citrate. Then, the PEG-DA with different molecular weights (550, 2k and 5k Da) were chelated onto the surface of the SPIO nanoparticles in water. The schematic preparation of PEGylated SPIO nanoparticles is shown in Figure S9. Nine PEGylated SPIO samples with different crystal sizes and PEG lengths were prepared. The particle size distribution of the PEGylated SPIO samples in aqueous solution was measured by DLS and is shown in Figure 2C. The average particle size was calculated and is shown in Table S1.

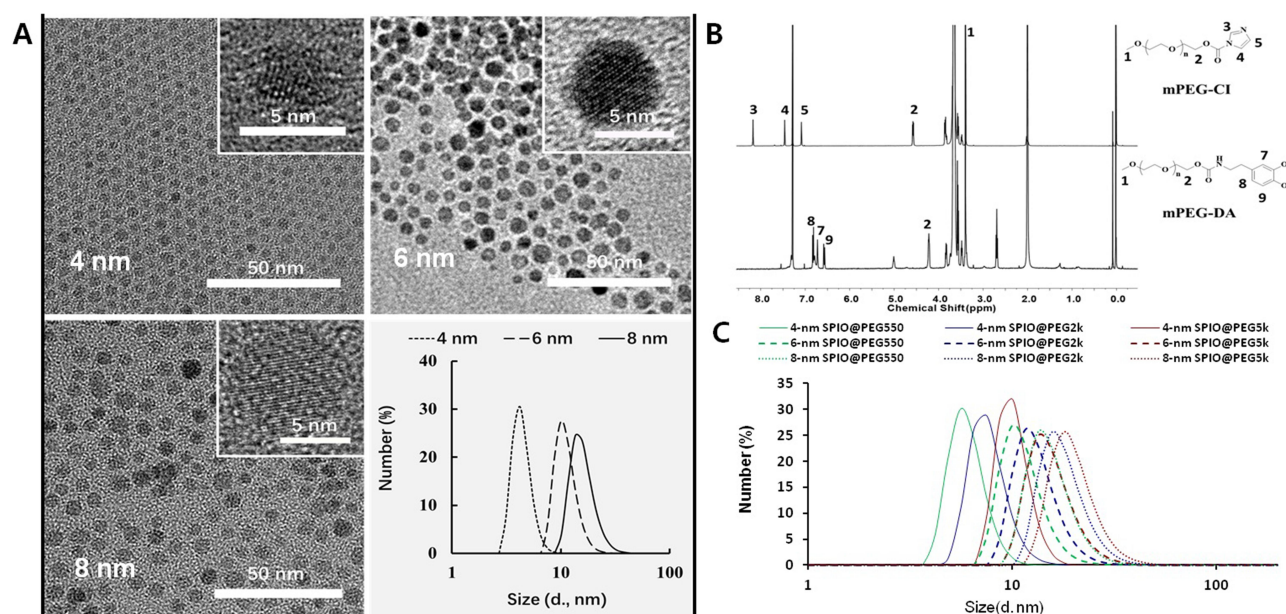**Figure 2** Size and PEG length-controlled PEGylated monocrystalline SPIO (SPIO@PEG) Nanocomposite. (**A**) TEM, HRTEM and DLS distribution of three SPIO nanocrystals (in hexane). (**B**) Chemical characterization of polyethylene glycol dopamine-modification. ^{1}H NMR spectra (CDCl$_3$) and characteristic peak assignment of activated intermediate (PEG-CI) and end product (PEG-DA). (**C**) DLS diameter distribution of the nine PEGylated SPIO nanoparticles in water.

Relaxivities of PEGylated SPIO at Different Magnetic Fields

Relaxivities (r_1 and r_2) of PEGylated SPIO were measured at three main magnetic fields (0.5 T, 1.5 T, and 3.0 T), and are listed in Table 1. r_1 and r_2 increased with an increase in the size of the SPIO nanocrystal, and this change is more sensitive for r_2 which results in an increase of the r_2/r_1 ratio. With the increasing molecular weight of PEG, r_1 and r_2 of the PEGylated SPIO nanoparticles also increase. Moreover, regular changes were observed at the three different magnetic fields. For all PEGylated SPIO, r_1 significantly reduced with the increase in the magnetic intensity, whereas r_2 slightly increased, leading to a sharp increase in the r_2/r_1 ratio.

Serum Stability and Cytotoxicity of PEGylated SPIO in vitro

We monitored the changes in the size of the nine PEGylated SPIO in DLS after incubation with 20% (v/v) fetal bovine serum (FBS) solution at 37°C for 24 h. All the data were statistically analyzed, and there were statistical differences among some of the data, but we further compared the mean (Number) and median (Intensity) of particle size at different time points and found no significant changes in the mean or median at each time point (4-nm SPIO@PEG550 as an example in Table S2A). However,

particle sizes over 100 nm gradually appeared over time (Figures S10–S12), though visible precipitation did not occur throughout the experiment. The cytotoxicity of PEGylated SPIO nanoparticles was evaluated by CCK-8 assay on the mouse macrophage cell line Raw 264.7. After being incubated with the nine PEGylated SPIO nanoparticles for 24 h, the cells were collected for visual inspection under a microscope. No observable morphological abnormalities were noted. Figures S13–S15 show the cytotoxicity of the nine PEGylated SPIO nanoparticles after incubation for 24 h. After statistical analysis, there was no statistically significant difference in cytotoxicity between different concentrations in nine samples (4-nm SPIO@PEG550 as an example in Table S2B, P = 0.256). The results suggest that the PEGylated SPIO nanoparticles possess reliable biocompatibility in our measured range (20-μg Fe/mL).

In vivo MRI Studies of PEGylated SPIO
CEMRA of SD Rats

CEMRA of SD rats was carried out on a clinical 3.0T MRI scanner, and the clinical used contrast agent (Magnevist) is used as control. Figure 3 and Figure S16 show the MR images of SD rats before and after intravenous injection of 4-nm SPIO@PEG5k, 6-nm SPIO@PEG5k, 8-nm SPIO@PEG5k nanoparticles, or Magnevist with the CEMRA sequence. The enhancement of angiography is seen for all but displays

Table I Relaxivities of Nine PEGylated SPIO Nanoparticles and Commercial Contrast Agent (Magnevist and Ferumoxytol) at Different Main Magnetic Fields

Sample	0.5 T			1.5 T			3.0 T		
	r_1 (mM^{-1} s^{-1})	r_2 (mM^{-1} s^{-1})	r_2/r_1	r_1 (mM^{-1} s^{-1})	r_2 (mM^{-1} s^{-1})	r_2/r_1	r_1 (mM^{-1} s^{-1})	r_2 (mM^{-1} s^{-1})	r_2/r_1
4-nm SPIO@PEG550[a]	14.2	24.6	1.73	11.5	35.5	3.08	6.99	41.5	5.94
4-nm SPIO@PEG2k[a]	13.5	22.5	1.67	11.4	30.9	2.71	7.57	33.1	4.38
4-nm SPIO@PEG5k[a]	16.1	28.0	1.74	14.2	40.5	2.85	8.82	46.2	5.24
6-nm SPIO@PEG550[a]	28.1	54.9	1.95	14.2	67.5	4.76	6.84	67.9	9.92
6-nm SPIO@PEG2k[a]	29.1	63.1	2.17	16.9	70.6	4.17	8.36	72.2	8.63
6-nm SPIO@PEG5k[a]	34.2	70.1	2.05	19.8	77.8	3.93	10.2	81.4	7.96
8-nm SPIO@PEG550[a]	41.6	102.7	2.47	17.2	117.1	6.81	7.94	119.4	15.1
8-nm SPIO@PEG2k[a]	45.3	111.0	2.45	19.0	122.0	6.42	8.60	129.5	15.1
8-nm SPIO@PEG5k[a]	47.3	118.1	2.49	20.0	130.1	6.52	10.1	141.4	14.0
Magnevist (GdDTPA)	3.72	4.29	1.15	3.56	4.08	1.15	3.58	3.96	1.11
Ferumoxytol[b]	38.0	85	2.24	19.9	60.8	3.06	10.0	62.3	6.23

Notes: [a]Measurement in this work, room temperature; [b]Data from Knobloch et al[38] and Questions and answers in MRI (http://mriquestions.com/ferumoxytol.html).[39]

different effects. High contrast imaging for an extended period (more than 2 h) is obtained in the 4-nm SPIO@PEG5k group, whereas the enhancement is relatively poor and quickly disappears in the other groups. The enhancement disappeared within 30 min in the 8-nm SPIO@PEG5k group, and disappeared within a few minutes in Magnevist group.

T$_1$-T$_2$ Dual-Mode MRI in Liver

Previous studies of relaxivity in vitro have found that 4-nm SPIO@PEG nanoparticles are a typical T_1-T_2 dual-mode contrast agent at 3.0 T (r_2/r_1= 5.24). To verify its validity in vivo, T_1-T_2 dual-mode MRI of SD rats was performed with a clinical 3.0 T MRI scanner. The SD rats liver underwent T_1WI and T_2WI in tandem before and after (1, 30, and 120 min) intravenous injection of 4-nm SPIO@PEG5k nanoparticles, with 8-nm SPIO@PEG5k nanoparticles as control. Figure 4 shows the images and corresponding NSI. The results show that the liver tissue reveals a hyperintensity in T_1WI and a hypointensity in T_2WI after administration of the 4-nm SPIO@PEG5k, and the hepatic vessels are visible. The

contrast enhancement effect lasts for more than 2 h in the T_1-T_2 dual-mode imaging. On administration of the 8-nm SPIO@PEG5k nanoparticles, there is only a slight enhancement in T_1WI at 1 min and a strong reduction in T_2WI.

MRI T$_2$ Mapping in Liver

Transverse T_2 mapping in liver of SD rats proceeded before and after administration of SPIO@PEG nanoparticles (Figure 5A). Figure 5B depicts the mean T_2 values of liver parenchyma at different time points and shows obvious changes, and T_2 maintained lower values for a prolonged time in both 4-nm SPIO@PEG5k and 8-nm SPIO@PEG5k groups.

Discussion

PEGylated SPIOs were developed over the past decades and may be the most promising alternative to GBCAs in MRI contrast agent. However, there was a lack of systematic study on the effects of particle size, PEG length, and magnetic field strength on its imaging. In our study, we
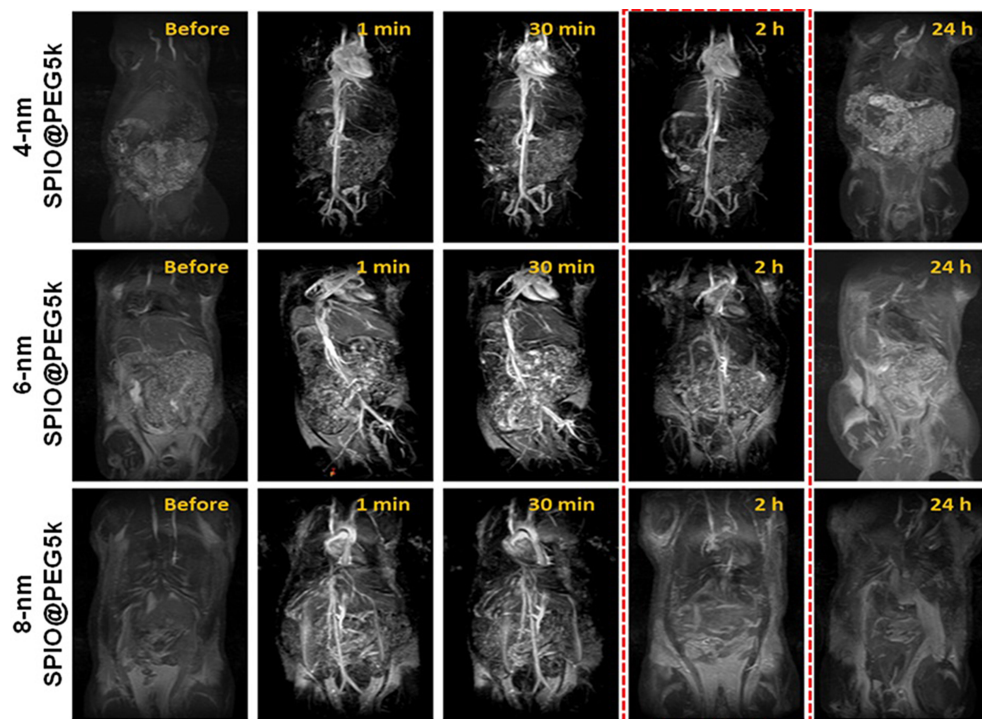
Figure 3 MRA images of SD rats before and after intravenous injection of SPIO@PEG nanoparticles. High contrast imaging more than 2 h is obtained in the 4-nm SPIO@PEG5k group.
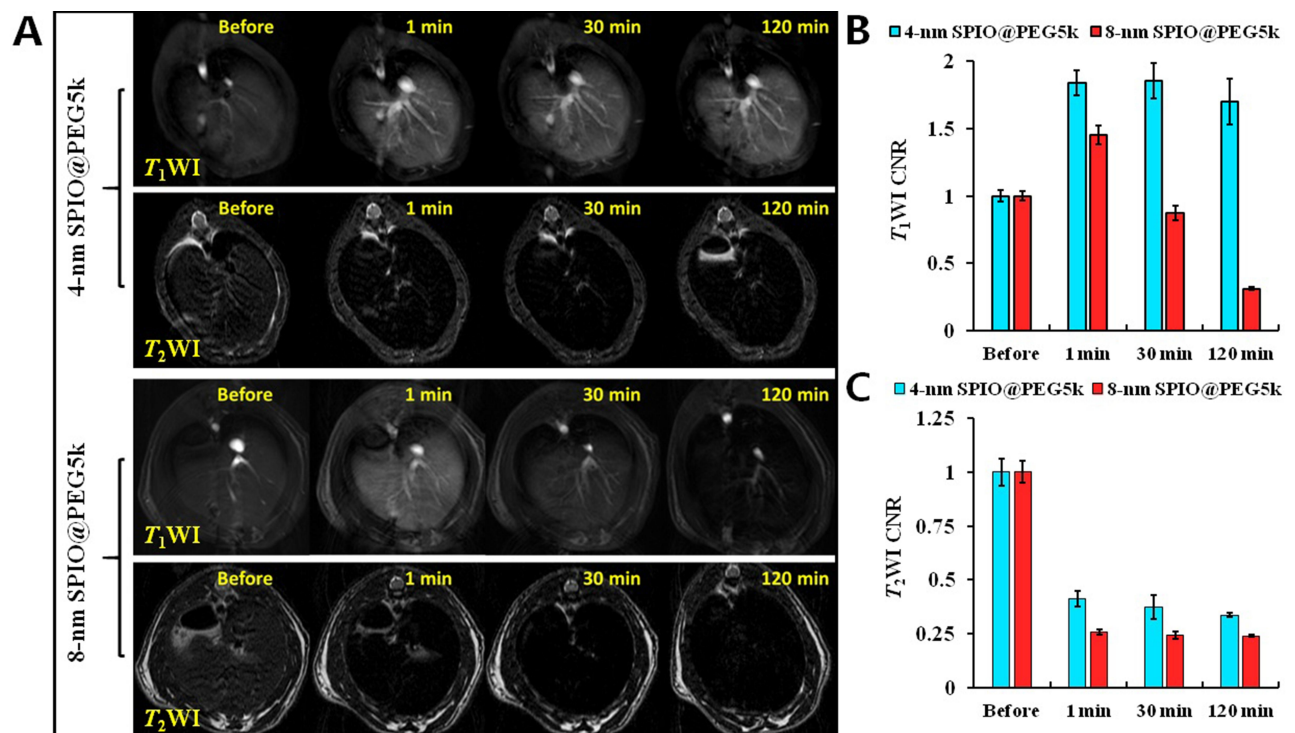

Figure 4 (**A**) SD rats hepatic T_1-T_2 dual-mode imaging before and after intravenous injection of 4-nm SPIO@PEG5k or 8-nm SPIO@PEG5k; (**B**) NSI in liver parenchyma on T_1WI; (**C**) NSI in liver parenchyma on T_2WI.
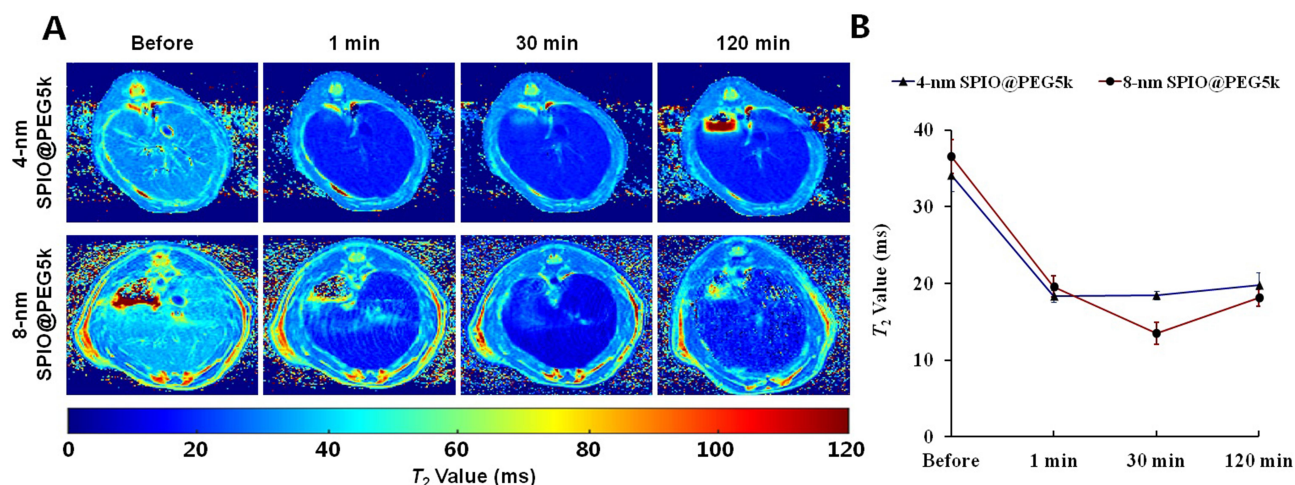
Figure 5 (**A**) Transverse T_2 mapping of SD rat liver, (**B**) Mean T_2 values in liver parenchyma before and after intravenous injection of 4-nm SPIO@PEG5k or 8-nm SPIO@PEG5k.

successfully prepared nine PEGylated monocrystalline SPIO with different crystal sizes and PEG lengths firstly, and then designed systematic experiments to study their performances and characteristics as MRI contrast agent.

To obtain PEGylated monodispersion SPIO, catechol-group modified PEG (mPEG-DA) was designed and coated on the surface of inorganic SPIO nanocrystals by the coordination of catechol and Fe^{3+} (Figure 1), which was commonly used in previous studies.[28,29] MPEG-DA was synthesized by a two-step chemical modification of mPEG-OH, and confirmed by ^1H NMR spectra of the activated intermediate and the final product. The characteristic peaks of PEG (1 and 2) and the imidazole ring (3, 4, and 5) appear together in the ^1H NMR spectrum of mPEG-CI showing the activation of the terminal hydroxyl group, and disappearance of the imidazole ring peaks and appearance of the dopamine peaks (7, 8, and 9) in the ^1H NMR spectrum of mPEG-DA (Figure 2B). Then, mPEG-DA with different molecular weights (550, 2k and 5k Da) were chelated onto the surface of three SPIO nanocrystals with different size, respectively, to obtain nine PEGylated SPIO samples with different crystal sizes and PEG lengths. These SPIO nanoparticles show narrow particle size distribution in the aqueous phase and the size increases with crystal size and the molecular weight of PEG-DA (Figure 2C). It demonstrated that the longer PEG molecules can create a thicker hydration layer on the surface of the SPIO nanocrystals.

T_1 relaxivity (r_1) and T_2 relaxivity (r_2) are the reciprocal of T_1 and T_2 relaxation time per unit concentration of contrast agents, and represent the net effectiveness of

shorter T_1 and T_2 relaxation times in MRI. r_2/r_1 ratio can be used to classify a contrast agent as a T_1, T_2, or T_1-T_2 dual-mode contrast agent in MRI enhancement application. Generally, T_1 contrast agents have a low r_2/r_1 ratio and can produce bright images in a T_1-weighted sequence, like paramagnetic chelates of gadolinium (Gd^{3+}), iron (Fe^{3+}), or manganese (Mn^{2+}) ions (r_2/r_1 ratio approximately equal to 1).[3] T_2 contrast agents possess a high r_2/r_1 ratio (greater than 10) and can produce dark images in a T_2 or T_2*-weighted sequence, like most of the magnetic nanoparticles.[13] The ideal T_1-T_2 dual-mode contrast agent should have an intermediate r_2/r_1 ratio (5 ~ 8), and hence can be used for contrast enhancement in T_1-T_2 dual-mode MRI.[30] Ferumoxytol is one of the SPIO commercial products with an average of 30 nm size. Its r_1, r_2 and r_2/r_1 are similar to the 6-nm SPIO sample synthesized in our study (Table 1), but the crystal shape and stability are not so excellent, on account of synthesized by coprecipitation method. Ferumoxytol is more likely to be captured by the reticuloendothelial system and has a shorter half-life of blood. Relaxivities of PEGylated SPIO at different magnetic fields show that the crystal size and the PEG length significantly influence the relaxivities of the PEGylated SPIO nanoparticles. The 8-nm SPIO@PEG5k has extremely high r_1 and r_2, is a good T_2 contrast agent at 3.0 T ($r_2/r_1 = 14.0$), is an ideal T_1-T_2 dual-mode contrast agent at 1.5 T ($r_2/r_1 = 6.52$), and is also an effective T_1 contrast agent at 0.5 T ($r_2/r_1 = 2.49$); 4-nm SPIO@PEG5k also has high r_1 and r_2, is T_1-T_2 dual-mode contrast agent at 3.0 T ($r_2/r_1 = 5.24$), and is a good T_1 contrast agent at 0.5 T ($r_2/r_1 = 1.74$) and 1.5 T ($r_2/r_1 = 2.85$). These results

indicate that it depends not only on the material itself but also on the main magnetic field strength for a contrast agent to be effective as T_1, T_2, or T_1-T_2 dual-mode contrast agent in MRI. However, this is often overlooked in previous reports. Consequently, the PEGylated SPIOs display good relaxivity but demonstrate different enhancement features. PEGylated SPIOs with different nanocrystal sizes and surface PEG lengths can be used as T_1, T_2, or T_1-T_2 dual-mode contrast agent at the appropriate magnetic field in MRI enhancement application.

The biodistribution and clearance of nanoparticles were heavily dependent on their stability and their interactions with proteins in plasma upon entering the bloodstream. Regarding serum stability test results of SPIO, statistical differences were found between some different sizes at different time. However, the differences had no clinical significance, because of the tiny change of mean particle sizes, which may be caused by attaching of major components of serum to SPIO, like proteins. PEGylated SPIO creates a PEG hydration layer on the surface of the SPIO nanocrystals, which can prevent non-specific binding to proteins in plasma. This is also an important factor impacting the imaging effect and characteristics for MRI nano contrast agents. In addition, all the nine PEGylated SPIO samples showed no statistical toxic effect on mouse macrophage cell line Raw 264.7, which suggested that PEGylated SPIO samples have good biological safety.

To evaluate the contrast enhancement of different PEGylated SPIO in vivo, three typical MR imaging sequences were used to study SD rats at a GE 3.0 T MRI scanner. CEMRA is an important clinical tool to detect cardiovascular diseases, such as vascular malformation, myocardial infarction, atherosclerotic plaque, and tumor angiogenesis.[31–34] Usually, the CEMRA sequence uses ultrashort TE and TR to enable a high T_1 weighting and to obtain high-resolution blood vessel imaging after administration of an intravenous T_1 contrast agent. The CEMRA of SD rats is consistent with the in vitro data, 4-nm SPIO@PEG5k is a T_1-T_2 dual-mode contrast agent, while 8-nm SPIO@PEG5k is only a T_2 contrast agent at 3.0 T. Another reason is that larger particles are more easily cleared by the reticuloendothelial system, which leads to a short circulation time for 8-nm SPIO@PEG5k. Therefore, 4-nm SPIO@PEG5k is more suitable for CEMRA in MRI. T_1-T_2 dual-mode MRI can easily produce an accurate match of spatial and temporal imaging parameters and provide cross-validation information.[35,36] As a result, it is routinely performed in clinical diagnostics. The results of T_1-T_2 dual-mode MRI in rats' liver confirm that the

4-nm SPIO@PEG5k can be used as a T_1-T_2 dual-mode contrast agent. However, the 8-nm SPIO@PEG5k is only a T_2 contrast agent at 3.0 T MRI. The T_2 value is a characteristic parameter of biological tissues, and accurate determination of the T_2 value is helpful to enhance disease detection and monitoring. It is used in dynamic contrast agent studies, diagnosis of epilepsy, and determination of the severity of Parkinson's disease in clinical practice.[37] These data of MRI T_2 mapping in rats' liver illustrate that 4-nm SPIO@PEG5k and 8-nm SPIO@PEG5k have specific liver distribution for a long period.

We successfully prepared nine PEGylated monocrystalline SPIO nanoparticles with different nanocrystal sizes and surface PEG lengths. All these PEGylated SPIO samples exhibit high relaxivities (r_1 and r_2) and have different enhancement features which are related to their crystal size and PEG length. The 8-nm SPIO@PEG5k is an effective T_2 contrast agent at 3.0 T ($r_2/r_1 = 14.0$), is an ideal T_1-T_2 dual-mode contrast agent at 1.5 T ($r_2/r_1 = 6.52$), and is also an effective T_1 contrast agent at 0.5 T ($r_2/r_1 = 2.49$). 4-nm SPIO@PEG5k is a T_1-T_2 dual-mode contrast agent at 3.0 T ($r_2/r_1 = 5.24$), and is a good T_1 contrast agent at 0.5 T ($r_2/r_1 = 1.74$) or 1.5 T ($r_2/r_1 = 2.85$). In MRI studies of SD rats at 3.0 T, 4-nm SPIO@PEG5k shows excellent contrast enhancement in MRA, T_1-T_2 dual-mode imaging, and T_2 mapping, whereas 8-nm SPIO@PEG5k only displays good enhancement in T_2WI and T_2 mapping.

Conclusions

In summary, PEGylated SPIOs synthesized in this study showed high T_1 and T_2 relaxivity, good biosafety and stability, and are the promising contrast agents in MRI. Furthermore, PEGylated SPIOs with different nanocrystal sizes and surface PEG lengths showed different imaging characteristics at various magnetic field intensity and can be used as T_1, T_2, or T_1-T_2 dual-mode contrast agents to meet the clinical demands of MRI at specific magnetic fields. Our results can provide a foundation for researchers in the selection of nanocrystal size, PEG length and magnetic field intensity for further study.

Abbreviations

GBCAs, gadolinium-based contrast agents; MRI, magnetic resonance imaging; NSF, nephrogenic system fibrosis; SPIO, Superparamagnetic iron oxides; PEG, polyethylene glycol; SNR, signal-to-noise ratio; CEMRI, contrast-enhanced MRI; AAS, atomic absorption spectrometer; PBS, phosphate-buffered saline; SD, Sprague Dawley;

SI, Signal intensity; NSI, normalized signal intensities; TEM, transmission electron microscopy; DLS, dynamic light scattering; HRTEM, high-resolution TEM; SAED, Selected area electron diffraction; FBS, fetal bovine serum.

Acknowledgment

Disclosure

The authors report there are no conflicts of interest to declare.

References

1. Fingerhut S, Sperling M, Holling M, et al. Gadolinium-based contrast agents induce gadolinium deposits in cerebral vessel walls, while the neuropil is not affected: an autopsy study. *Acta Neuropathol*. 2018;136(1):127–138. doi:10.1007/s00401-018-1857-4
2. Kanda T, Fukusato T, Matsuda M, et al. Gadolinium-based contrast agent accumulates in the brain even in subjects without severe renal dysfunction: evaluation of autopsy brain specimens with inductively coupled plasma mass spectroscopy. *Radiology*. 2015;276(1):228–232. doi:10.1148/radiol.2015142690
3. Runge VM, Heverhagen JT. Advocating the development of next-generation high-relaxivity gadolinium chelates for clinical magnetic resonance. *Invest Radiol*. 2018;53:381–389.
4. Laurent S, Forge D, Port M, et al. Magnetic iron oxide nanoparticles: synthesis, stabilization, vectorization, physicochemical characterizations, and biological applications. *Chem Rev*. 2008;108 (6):2064–2110. doi:10.1021/cr068445e
5. Lee SH, Kim BH, Na HB, Hyeon T. Paramagnetic inorganic nanoparticles as T1 MRI contrast agents. *Wiley Interdiscip Rev Nanomed Nanobiotechnol*. 2014;6(2):196–209. doi:10.1002/wnan.1243
6. Wang Y-XJ. Superparamagnetic iron oxide based MRI contrast agents: current status of clinical application. *Quant Imaging Med Surg*. 2011;1(1):35–40.
7. Xie J, Liu G, Eden HS, Ai H, Chen X. Surface-engineered magnetic nanoparticle platforms for cancer imaging and therapy. *Acc Chem Res*. 2011;44(10):883–892. doi:10.1021/ar200044b
8. Su H-Y, Wu C-Q, Li D-Y, Ai H. Self-assembled superparamagnetic nanoparticles as MRI contrast agents— a review. *Chin Phys B*. 2015;24:12. doi:10.1088/1674-1056/24/12/127506
9. Fu J, Fiegel J, Krauland E, Hanes J. New polymeric carriers for controlled drug delivery following inhalation or injection. *Biomaterials*. 2002;23(22):4425–4433. doi:10.1016/S0142-9612(02)00182-5
10. Cheng T-C, Chuang K-H, Chen M, et al. Sensitivity of PEGylated interferon detection by anti-polyethylene glycol (PEG) antibodies depends on PEG length. *Bioconjug Chem*. 2013;24(8):1408–1413. doi:10.1021/bc3006144
11. Knop K, Hoogenboom R, Fischer D, Schubert US. Poly(ethylene glycol) in drug delivery: pros and cons as well as potential alternatives. *Angew Chem Int Ed*. 2010;49(36):6288–6308. doi:10.1002/anie.200902672
12. Seifert O, Pollak N, Nusser A, et al. Immuno-LipoTRAIL: targeted delivery of TRAIL-functionalized liposomal nanoparticles. *Bioconjug Chem*. 2014;25(5):879–887. doi:10.1021/bc400517j
13. Ai H, Flask C, Weinberg B, et al. Magnetite-loaded polymeric micelles as ultrasensitive magnetic-resonance probes. *Adv Mater*. 2005;17(16):1949–1952. doi:10.1002/adma.200401904
14. Li L, Wu C, Pan L, et al. Bombesin-functionalized superparamagnetic iron oxide nanoparticles for dual-modality MR/NIRFI in mouse models of breast cancer. *Int J Nanomedicine*. 2019;14:6721–6732. doi:10.2147/IJN.S211476
15. Nasongkla N, Shuai X, Ai H, et al. cRGD-functionalized polymer micelles for targeted doxorubicin delivery. *Angew Chem Int Ed Engl*. 2004;43(46):6323–6327. doi:10.1002/anie.200460800
16. Amstad E, Gillich T, Bilecka I, Textor M, Reimhult E. Ultrastable iron oxide nanoparticle colloidal suspensions using dispersants with catechol-derived anchor groups. *Nano Lett*. 2009;9(12):4042–4048. doi:10.1021/nl902212q
17. Kim BH, Lee N, Kim H, et al. Large-scale synthesis of uniform and extremely small-sized iron oxide nanoparticles for high-resolution T1 magnetic resonance imaging contrast agents. *J Am Chem Soc*. 2011;133(32):12624–12631. doi:10.1021/ja203340u
18. Na HB, Palui G, Rosenberg JT, Ji X, Grant SC, Mattoussi H. Multidentate catechol-based polyethylene glycol oligomers provide enhanced stability and biocompatibility to iron oxide nanoparticles. *ACS Nano*. 2012;6(1):389–399. doi:10.1021/nn203735b
19. Sandiford L, Phinikaridou A, Protti A, et al. Bisphosphonate-anchored PEGylation and radiolabeling of superparamagnetic iron oxide: long-circulating nanoparticles for in vivo multimodal (T1 MRI-SPECT) imaging. *ACS Nano*. 2013;7(1):500–512. doi:10.1021/nn3046055
20. Bulte JWM, Kraitchman DL. Iron oxide MR contrast agents for molecular and cellular imaging. *NMR Biomed*. 2004;17(7):484–499. doi:10.1002/nbm.924
21. Lee N, Yoo D, Ling D, Cho MH, Hyeon T, Cheon J. Iron oxide based nanoparticles for multimodal imaging and magnetoresponsive therapy. *Chem Rev*. 2015;115(19):10637–10689. doi:10.1021/acs.chemrev.5b00112
22. Bai C, Jia Z, Song L, et al. Time-dependent T1–T2 switchable magnetic resonance imaging realized by c(RGDyK) modified ultra-small Fe3O4 nanoprobes. *Adv Funct Mater*. 2018;28(32):1802281. doi:10.1002/adfm.201802281
23. Zhou Z, Bai R, Munasinghe J, Shen Z, Nie L, Chen X. T1-T2 dual-modal magnetic resonance imaging: from molecular basis to contrast agents. *ACS Nano*. 2017;11(6):5227–5232. doi:10.1021/acsnano.7b03075
24. Cai Z, Wu C, Yang L, Wang D, Ai H. Assembly-controlled magnetic nanoparticle clusters as MRI contrast agents. *ACS Biomater Sci Eng*. 2020. doi:10.1021/acsbiomaterials.9b01198
25. Demortière A, Panissod P, Pichon BP, et al. Size-dependent properties of magnetic iron oxide nanocrystals. *Nanoscale*. 2011;3 (1):225–232. doi:10.1039/C0NR00521E
26. Tong S, Hou S, Zheng Z, Zhou J, Bao G. Coating optimization of superparamagnetic iron oxide nanoparticles for high T2 relaxivity. *Nano Lett*. 2010;10(11):4607–4613. doi:10.1021/nl102623x
27. Sun S, Zeng H, Robinson DB, et al. Monodisperse MFe2O4 (M = Fe, Co, Mn) nanoparticles. *J Am Chem Soc*. 2004;126(1):273–279. doi:10.1021/ja0380852
28. Li Y, Wen J, Qin M, Cao Y, Ma H, Wang W. Single-molecule mechanics of catechol-iron coordination bonds. *ACS Biomater Sci Eng*. 2017;3(6):979–989. doi:10.1021/acsbiomaterials.7b00186
29. Xu C, Xu K, Gu H, et al. Dopamine as a robust anchor to immobilize functional molecules on the iron oxide shell of magnetic nanoparticles. *J Am Chem Soc*. 2004;126(32):9938–9939. doi:10.1021/ja0464802

30. Zhou Z, Zhao Z, Zhang H, et al. Interplay between longitudinal and transverse contrasts in Fe3O4 nanoplates with (111) exposed surfaces. *ACS Nano*. 2014;8(8):7976–7985. doi:10.1021/nn5038652

31. Jain R, Sawhney S. Contrast-enhanced MR angiography (CE-MRA) in the evaluation of vascular complications of renal transplantation. *Clin Radiol*. 2005;60(11):1171. doi:10.1016/j.crad.2005.05.004

32. Svensson J. Contrast-enhanced magnetic resonance angiography. *Acta Radiol*. 2015;44(s429):1–30. doi:10.1034/j.1600-0455.44.s.429.1.x

33. Wu C, Li D, Yang L, et al., Multivalent manganese complex decorated amphiphilic dextran micelles as sensitive MRI probes. *J Mater Chem B*. 2015;8:1470–1473. doi:10.1039/C4TB02036G

34. Wu C, Yang L, Chen Z, et al. Poly(ethylene glycol) modified Mn2+ complexes as contrast agents with a prolonged observation window in rat MRA. *RSC Adv*. 2017;7(86):54603–54609. doi:10.1039/c7ra09975d

35. Shin T-H, Choi J-S, Yun S, et al. T1 and T2 dual-mode MRI contrast agent for enhancing accuracy by engineered nanomaterials. *ACS Nano*. 2014;8(4):3393–3401. doi:10.1021/nn405977t

36. Zhou Z, Wu C, Liu H, et al. Surface and interfacial engineering of iron oxide nanoplates for highly efficient magnetic resonance angiography. *ACS Nano*. 2015;9(3):3012–3022. doi:10.1021/nn507193f

37. Deoni SCL, Rutt BK, Peters TM. Rapid combined T1 and T2 mapping using gradient recalled acquisition in the steady state. *Magn Reson Med*. 2003;49(3):515–526. doi:10.1002/mrm.10407

38. Knobloch G, Colgan T, Wiens CN, et al. Relaxivity of Ferumoxytol at 1.5 T and 3.0 T. *Invest Radiol*. 2018;53(5):257–263. doi:10.1097/RLI.0000000000000434

39. Questions and answers in MRI. Available from: http://mriquestions.com/ferumoxytol.html.